THE JOURNAL OF PHYSICAL CHEMISTRY Letters

Letter

pubs.acs.org/JPCL

Anharmonic Theoretical Vibrational Spectroscopy of Polypeptides

Paweł T. Panek and Christoph R. Jacob*

Institute of Physical and Theoretical Chemistry, TU Braunschweig, Hans-Sommer-Str. 10, 38106 Braunschweig, Germany

Supporting Information

ABSTRACT: Because of the size of polypeptides and proteins, the quantum-chemical prediction of their vibrational spectra presents an exceptionally challenging task. Here, we address one of these challenges, namely, the inclusion of anharmonicities. By performing the expansion of the potential energy surface in localized-mode coordinates instead of the normal-mode coordinates, it becomes possible to calculate anharmonic vibrational spectra of polypeptides efficiently and reliably. We apply this approach to calculate the infrared, Raman, and Raman optical activity spectra of helical alanine polypeptides consisting of up to 20 amino acids. We find that while anharmonicities do not alter the band shapes, simple scaling procedures cannot account for the different shifts found for the individual bands. This closes an important gap in theoretical vibrational spectroscopy by making it possible to quantify the anharmonic contributions and opens the door to a *first-principles* calculation of multidimensional vibrational spectra.

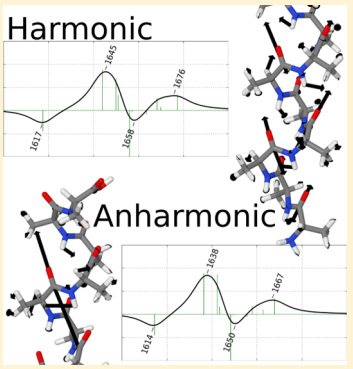

Vibrational spectroscopy is an essential experimental technique for probing the fast structural dynamics of biomolecules such as polypeptides and proteins.[1,2] In addition to conventional infrared (IR) and Raman spectroscopy, specialized techniques such as their chiral variants, vibrational circular dichroism (VCD), and Raman optical activity (ROA), as well as methods such as resonance Raman spectroscopy and two-dimensional infrared (2D-IR) spectroscopy play a major role, because these can provide more specific structural information.[3,4]

For the interpretation of such vibrational spectra and for extracting structural information from them, theoretical modeling is generally mandatory.[5] This is particularly true for specialized techniques such as VCD and ROA for which simple empirical rules are lacking. However, the *first-principles* prediction of vibrational spectra of polypeptides and proteins with quantum-chemical methods presents an exceptionally challenging task.

First, polypeptides and proteins consist of hundreds to thousands of atoms, which results in a considerable computational effort already for the calculation of the *harmonic* vibrational spectrum for a single structure.[6] For methods other than IR, an additional effort is required for the calculation of the property tensor derivatives that determine the vibrational intensities.[5] This usually restricts the quantum-chemical treatment to density-functional theory (DFT), which in turn introduces inaccuracies due to the use of approximate exchange−correlation functionals. Second, the inclusion of solvation effects is essential for polypeptides and proteins in solution but is feasible only with simplified implicit or explicit solvation models.[7] Third, accounting for the conformational flexibility of polypeptides and proteins requires calculations for many different structures from a suitably generated ensemble.[8,9]

While methods tackling some of these challenges have been developed,[10−14] the inclusion of anharmonic corrections in the quantum-chemical calculation of vibrational spectra of polypeptides and proteins has not been addressed to date. Instead, vibrational spectra calculated in the harmonic approximation are corrected by applying a scaling factor.[15,16] However, it remains unclear how anharmonic corrections affect vibrational spectra of polypeptides and proteins and whether simple scaling procedures are justified. In particular for chiral vibrational spectroscopies, anharmonic corrections could significantly alter band shapes and the observed intensity patterns.[17] Because the lack of anharmonicities is only one of the shortcomings of harmonic vibrational calculations for polypeptides and protein, its significance cannot be assessed by comparing calculated harmonic spectra directly to experiment, but computational studies comparing calculated harmonic and anharmonic spectra are required.

On the other hand, for small molecules with up to 10−20 atoms, anharmonic vibrational spectra can be calculated with an incredible accuracy of up to 1 cm^{-1} for the fundamental vibrations by combining high-accuracy potential energy surfaces with state-of-the-art methods, in particular, vibrational self-consistent field (VSCF) plus vibrational configuration interaction (VCI) and vibrational coupled cluster (VCC) theory, for solving the vibrational Schrödinger equation.[18−20] The importance of anharmonicities for achieving a satisfactory agreement with experiment is well-established for such small molecules[21] and has been assessed for dipeptides.[22] It has been shown that anharmonicities can have a significant effect on the intensity patterns observed in chiral vibrational spectroscopies.[23,24] More approximate perturbative methods allow for the inclusion of anharmonicities for medium-sized molecules

Received: June 30, 2016
Accepted: July 26, 2016

DOI: 10.1021/acs.jpclett.6b01451
J. Phys. Chem. Lett. 2016, 7, 3084−3090

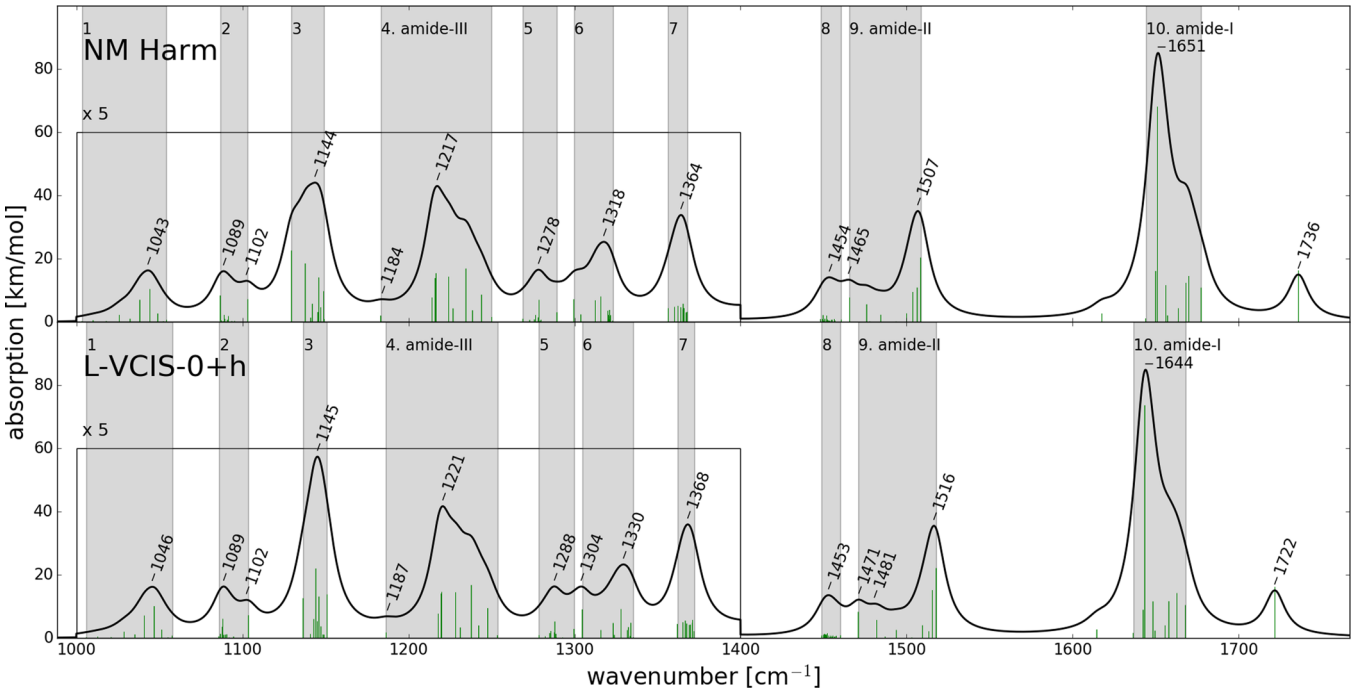

Figure 1. Infrared spectrum of 3_{10}-Ala_{10} calculated in the double-harmonic approximation (upper panel) and including anharmonic contributions, for the potential energy and dipole moment surfaces, using the L-VCIS-0+h model (lower panel). All calculations have been performed using DFT/BP86/TZVP. The assignment of the modes to vibrational bands used in the localization is indicated with gray boxes (see the Supporting Information for detailed assignment).

with up to about 50 atoms,[25,26] but the steep scaling of the computational costs puts a treatment of anharmonic corrections for polypeptides and proteins with such methods out of reach.

This Letter aims at closing this apparent gap between the possibility of a highly accurate prediction of anharmonicities for small molecules and their complete neglect or highly empirical treatment for polypeptides and proteins. Through the expansion of the potential energy surface required for the prediction of anharmonic vibrational spectra in localized modes instead of normal modes, an efficient yet reliable treatment becomes possible.[27,28] Here, we apply this localized-mode VSCF/VCI (L-VSCF/L-VCI) method to the test case of helical alanine polypeptides to demonstrate its applicability to polypeptides and to investigate the impact of anharmonic corrections on their IR, Raman, and ROA spectra.

The calculation of anharmonic vibrational spectra is commonly based on the *n*-mode expansion of the potential energy surface[29,30]

$$V(q_1, \cdots, q_M) = \sum_{i=1}^{M} V_i^{(1)}(q_i) + \sum_{\substack{i,j=1 \\ i\neq j}}^{M} V_{ij}^{(2)}(q_i, q_j) + \sum_{\substack{i,j,k=1 \\ i\neq j\neq k}}^{M} V_{ijk}^{(3)}(q_i, q_j, q_k) + \cdots \quad (1)$$

where M is the number of considered modes and $V_i^{(1)}(q_i)$, $V_{ij}^{(2)}(q_i, q_j)$, $V_{ijk}^{(3)}(q_i, q_j, q_k)$, and so on are one-mode, two-mode, three-mode, and higher-order contributions. In anharmonic calculations for small molecules, this expansion is usually performed in terms of the normal-mode coordinates, q_i, up to a certain order. However, these normal modes in polypeptides and proteins are in general very delocalized,[31] which results in large anharmonic couplings (two-mode and higher-oder potentials) between normal modes and a very slow convergence of the *n*-mode expansion and, in turn, of the VCI expansion[27,28] (for related work, see also refs 32−36).

We have previously shown that an efficient treatment of anharmonicities is possible by performing a transformation from normal modes to rigorously defined localized modes.[27,31] Thus, we perform the *n*-mode expansion with respect to localized-mode coordinates, $\tilde{q}_i$, instead of the normal-mode coordinates, q_i. We then truncate this expansion at second order and introduce additional approximations for the two-mode potentials

$$V(\tilde{q}_1, \cdots, \tilde{q}_M) = \sum_{i=1}^{M} \tilde{V}_i^{(1)}(\tilde{q}_i) + \sum_{\substack{i,j=1 \\ i\neq j}}^{M} \tilde{H}_{ij}\tilde{q}_i\tilde{q}_j + \sum_{(i,j)\in\mathcal{N}} \tilde{V}_{ij}^{(2,a)}(\tilde{q}_i, \tilde{q}_j) \quad (2)$$

Here, the first term contains the one-mode potentials, which are calculated on a grid of 16 points along each localized-mode coordinate. The second term describes the harmonic part of the two-mode potentials, which arises because the Hessian matrix with respect to localized-mode coordinates, $\tilde{H}_{ij} = \frac{\partial^2 E_{pot}}{\partial\tilde{q}_i\partial\tilde{q}_j}$, is not diagonal. However, this contribution does not require any additional computational effort compared to the harmonic approximation and is thus included for all pairs of modes. Finally, the third term contains the anharmonic contributions to the two-mode potentials $\tilde{V}_{ij}^{(2,a)}(\tilde{q}_i, \tilde{q}_j)$, which are calculated explicitly on grids of 16 × 16 points[27] using DFT/BP86/TZVP (see Computational Methods for details). Here, these anharmonic two-mode potentials are included only for relevant

DOI: 10.1021/acs.jpclett.6b01451
J. Phys. Chem. Lett. 2016, 7, 3084−3090

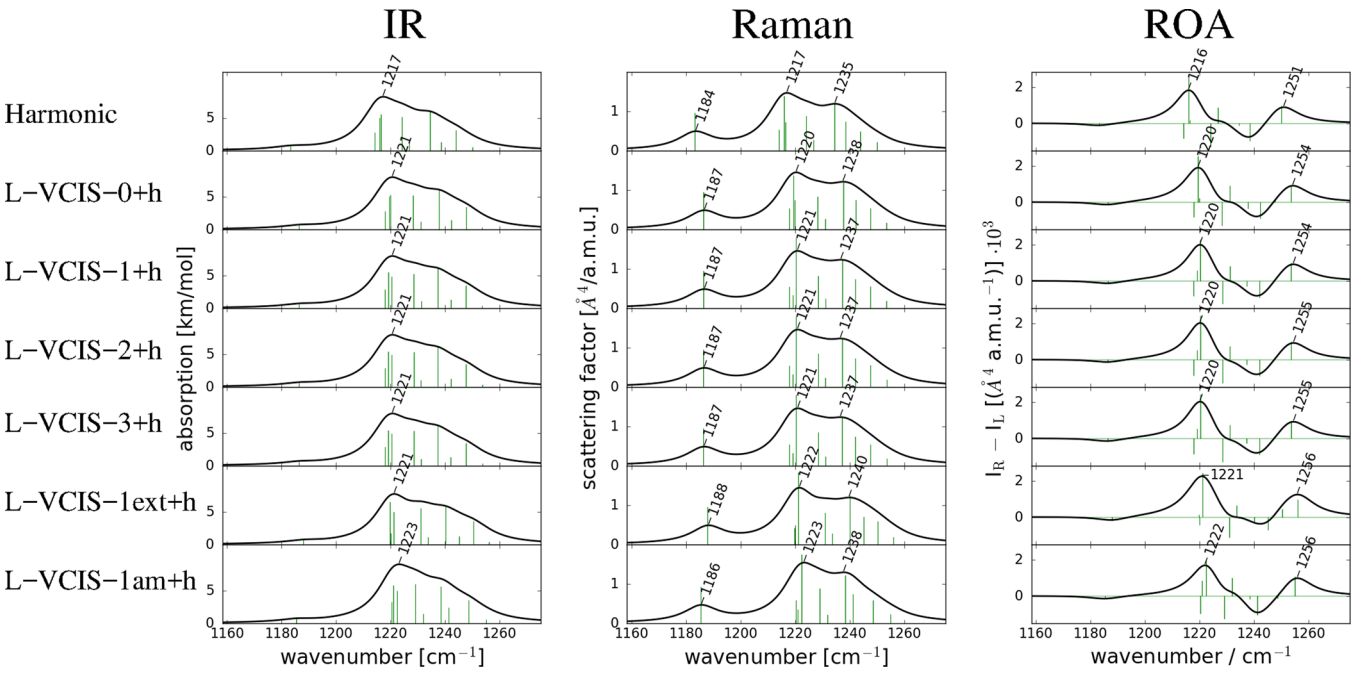

Figure 2. Comparison of the amide III band of 3_{10}-Ala_{10} calculated in the double-harmonic approximation and by including anharmonic corrections using different models with DFT/BP86/TZVP. See text for description of the different models.

pairs of modes, collected in the subset $\mathcal{N}$ (see below for details).

With this expansion for the potential-energy surface, the vibrational Schrödinger equation is solved using L-VSCF/L-VCI, as described in refs 27 and 28. For the IR spectra, the electronic anharmonicities are included by using an *n*-mode expansion of the dipole moment surface that mirrors the one used for the potential energy surface. For Raman and ROA, the required polarizability tensor surfaces would introduce a significant additional computational effort. Therefore, for Raman and ROA the intensities are treated by assuming that these polarizability tensors depend linearly on the nuclear displacements. Further details on the calculation of the IR, Raman, and ROA intensities are given in the Supporting Information.

As a first test case, we consider a decaalanine polypeptide in its 3_{10}-helical conformation, denoted 3_{10}-Ala_{10} in the following. Previously,[27] we have investigated the applicability of L-VSCF/L-VCI calculations for the amide I and II bands in helical Ala_6 and found that the L-VCIS-0+h model, in which only anharmonic one-mode potentials and harmonic two-mode potentials are included (i.e., all anharmonic two-mode potentials in the third term of eq 2 are neglected), can serve as an efficient and accurate approximation for including anharmonicity in vibrational calculations for polypeptides. To apply this model, the normal modes are assigned to bands as described in ref 37, and a unitary transformation of the modes within each of these bands is performed to arrive at maximally localized modes. Further details on the assignment are given in the Supporting Information.

In our calculations we are considering the spectral region between 1100 and 1800 cm^{-1} consisting of 111 normal modes, in which the most important bands for polypeptides and proteins vibrational spectroscopy can be found. The construction of the anharmonic one-mode potentials expanded on 16-point grids then requires 1776 single-point energy calculations. If we want to include anharmonic two-mode potentials within each subset of localized modes, another 11 520 single-point (SP) energy calculations would be required. On top of that, including all two-mode couplings between different bands in the considered region of the spectrum requires 1 551 360 additional SP calculations. Thus, for 3_{10}-Ala_{10} the L-VCIS-0+h model reduces the computational effort by 3 orders of magnitude.

The infrared spectrum obtained with the L-VCIS-0+h model in the spectral region between 1100 and 1800 cm^{-1} is shown in the lower panel of Figure 1. For comparison, the upper panel of Figure 1 shows the spectrum calculated in the double-harmonic approximation. Overall, the calculated harmonic and the anharmonic spectra are very similar, and the main difference is a shift of the bands from the harmonic to the anharmonic spectra. However, this shift is not uniform but differs for each of the bands. For the amide I band, the maximum is shifted from 1651 to 1644 cm^{-1}, which resembles the behavior often modeled with an empirical scaling of the calculated harmonic spectrum. On the other hand, the maximum of the amide II band shifts from 1507 to 1516 cm^{-1}, i.e., in the opposite direction. Similarly, for the lower-wavenumber features at 1465 and 1479 cm^{-1}, a small, yet not uniform, blue shift is observed. For the amide III band, the anharmonicity does not influence the shape of the band, but again in the L-VCIS-0+h model a shift toward higher wavenumbers is observed, namely to 1221 cm^{-1}. Finally, for the skeletal C−N-stretching region (band 3 in Figure 1), the band is only slightly shifted, but a rather pronounced change of the band shape is observed. The fact that anharmonicities can result in a shift of certain features to higher wavenumbers might at first seem surprising. It is mostly due to the fact that the anharmonicities can affect modes belonging to one band of the spectrum differently, resulting in an apparent shift of the peak maximum.

Thus, the LVCI-S-0+h model makes it possible to include anharmonicities in the calculation of the vibrational spectra of 3_{10}-Ala_{10} at a reasonable computational cost and predicts some changes in the infrared spectra that could not be obtained from

DOI: 10.1021/acs.jpclett.6b01451
J. Phys. Chem. Lett. 2016, 7, 3084−3090

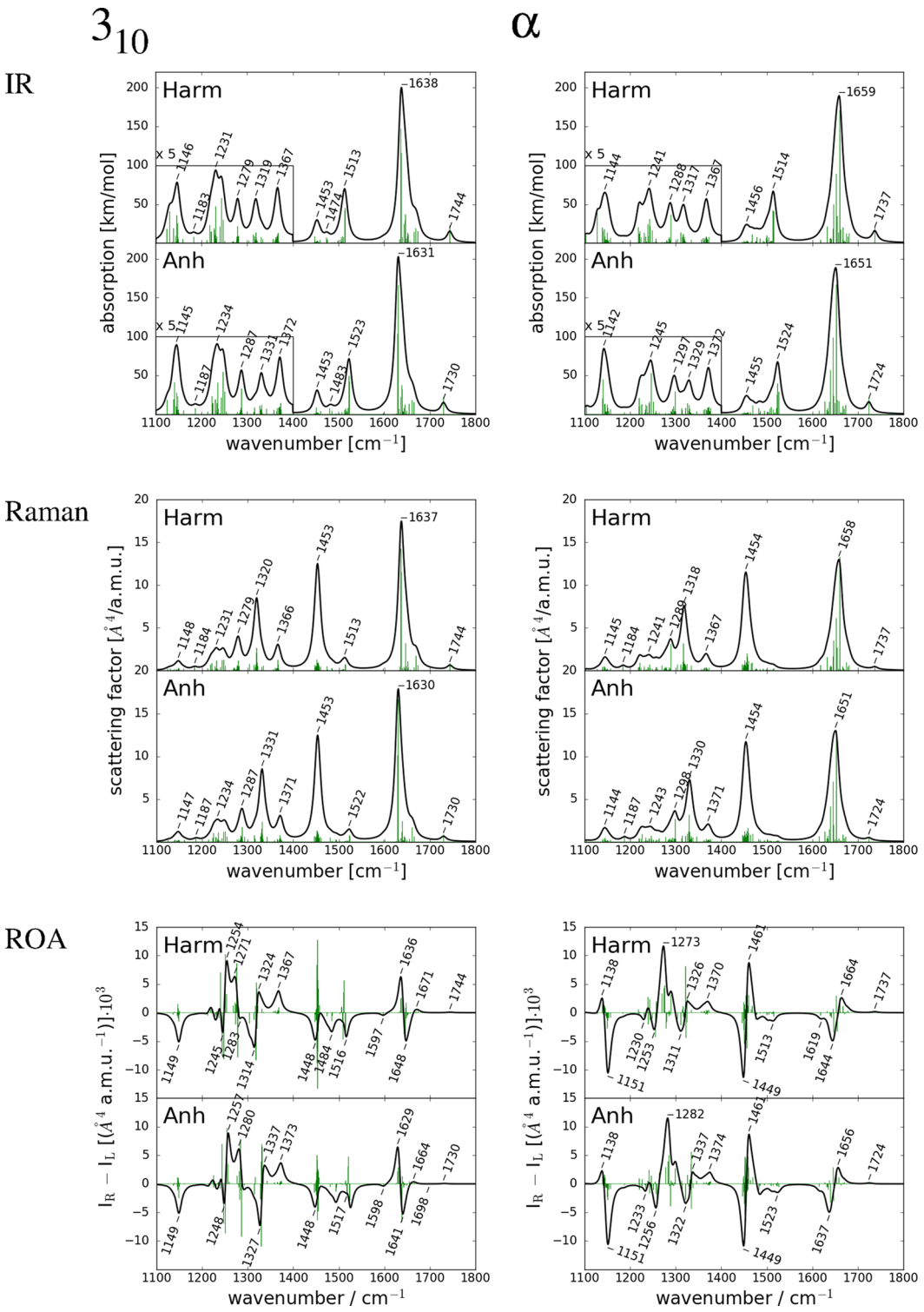

Figure 3. Calculated IR, Raman, and ROA spectra of Ala_{20} in a 3_{10}-helical conformation (left) and an α-helical conformation (right). All calculations have been performed using DFT/BP86/TZVP. In each panel, the upper part shows the spectrum calculated in the double-harmonic approximation, while the lower panel shows the calculated spectrum including anharmonic contributions within the L-VCIS-0+h model.

a simple scaling procedure as it is usually applied. Nevertheless, the infrared spectrum remains qualitatively unchanged and the differences are, while non-negligible, in general rather subtle.

In the investigated model, L-VCIS-0+h, we include only the harmonic two-mode potential arising from the localization of the normal modes. The validity of this approximation can be assessed by successive inclusion of additional anharmonic two-mode potentials explicitly in the last term of eq 2. It has been shown previously[27,32] that the mutual couplings of localized modes exhibit a decay with the distance between the centers of the localized modes. Therefore, additional couplings can be included based on this distance.

To confirm the applicability of the simplified L-VCIS-0+h model, we investigate the influence of including additional

DOI: 10.1021/acs.jpclett.6b01451
J. Phys. Chem. Lett. 2016, 7, 3084−3090

explicit anharmonic two-mode potentials on amide III band. The IR, Raman, and ROA spectra calculated for the amide III band with different models are compared in Figure 2. As already observed for the IR spectrum (cf. Figure 1), the L-VCIS-0+h model leads to a small shift of the amide III band toward higher wavenumbers; however, the band shape remains unchanged for all three types of spectra. If the anharmonic two-mode couplings between the amide III localized modes on one, two, or three nearest-neighbor residues are included in the L-VCIS-1+h, L-VCIS-2+h, and L-VCIS-3+h models, respectively, no further change of the spectra is observed. As the third-nearest neighbor corresponds to one full turn of the 3_{10}-helix, we expect that including additional two-mode couplings will have no further effect.

In addition, we have also included couplings of the localized amide III modes with localized modes of other bands. First, in the L-VCIS-1ext+h model, for each localized amide III mode its anharmonic couplings to the amide III as well as the C−H-bending localized modes (bands 5 and 6 in Figure 1) on the same and on the neighboring residues are included. Thus, all nearest-neighbor couplings within the extended amide III region[38] are included. Second, in the L-VCIS-1am+h model, for each localized amide III mode its anharmonic couplings to the amide I, amide II, and amide III localized modes on the same and on the neighboring residues are included. Both these models result in IR, Raman, and ROA spectra that are largely identical to those obtained with L-VCIS-0+h. Some slight changes in the band shapes, such as a change of the negative feature at ca. 1240 cm^{-1}, can be noticed only for the ROA spectra. Finally, we also note that L-VCIS is indeed sufficient in all the cases considered here, as is show in the Supporting Information by comparing to L-VCISD and L-VCISDT, which result in identical spectra for the models considered here.

Having established the applicability of the L-VCIS-0+h model for the vibrational spectra of polypeptides, we turn to a second example, namely, dodecaalanine Ala_{20} in an 3_{10}-helical and in an α-helical conformation. The IR, Raman, and ROA spectra of these models have been studied previously in refs 17 and 39, and the assignment of the normal modes to vibrational bands used here is the one established previously (see the Supporting Information for further details).

The calculated anharmonic IR, Raman, and ROA spectra obtained with the L-VCIS-0+h model for both helical conformations in the spectral region between 1000 and 1700 cm^{-1} are presented in Figure 3, alongside the corresponding spectra calculated in the double-harmonic approximation. For Ala_{20}, the calculation of the anharmonic one-mode potentials for all modes in this spectral region required 2912 single-point energy calculations. Including the anharmonic two-mode couplings within each band would require an additional 515 840 single-point energy calculations, whereas including all anharmonic two-mode couplings within the considered spectral region would require 4 216 576 additional single-point energy calculations.

Overall, the harmonic and anharmonic vibrational spectra shown in Figure 3 are qualitatively rather similar in all cases. Most significant is the shift of certain bands when going from the harmonic to the anharmonic spectrum. The largest shift is found for the amide I band, which shifts from 1638 to 1624 cm^{-1} in the 3_{10}-helical conformation and from 1659 to 1645 cm^{-1} in the α-helical conformations. For other bands, in particular the amide II band (at ca. 1513−1514 cm^{-1}) and for the C−H-bending bands (at ca. 1275−1325 cm^{-1}), a small shift to larger wavenumbers is found. The remaining bands hardly change when going from the harmonic to the anharmonic calculations. Looking at the ROA spectra, the inclusion of anharmonicities introduces only rather small and subtle changes to the band shapes and the intensity patterns that are hardly visible. All the features that are characteristic for the specific helical conformations, such as the inverted amide I couplet,[37,39] are not affected by the inclusion of anharmonicities.

In summary, we find that anharmonic corrections have only a minor effect on the IR, Raman, and ROA spectra of polypeptides. They do not alter the band shapes significantly, which is an important observation in particular for ROA spectroscopy where the band shapes intricately depend on the mechanical and electronic coupling of local vibrations.[39] The main effect of anharmonic corrections is a shift of some parts of the spectrum. However, this shift is not uniform but specific for each vibrational band. These effects cannot be reproduced with the empirical scaling methods commonly used.

Here, we have demonstrated that the efficient L-VCIS-0+h model is suitable for include these effects from *first-principles*, without the need to introduce empirical scaling parameters. Thus, this computational model can provide a reliable estimate of the impact of anharmonicities on the vibrational spectra of polypeptides. Moreover, its accuracy can be systematically validated by successively including the most important anharmonic two-mode couplings explicitly. The additional computational effort required by the L-VCIS-0+h model is comparable to and exhibits the same scaling as the calculation of the harmonic Raman or ROA spectra. Finally, the decay of the couplings between localized modes makes it possible to assess the reliability of the L-VCIS-0+h model by successively including additional couplings, as has been done here for Ala_{10} (cf. Figure 2).

Of course, the simple and efficient L-VCIS-0+h model as applied here has some remaining limitations. First, the coupling between different vibrational bands has been neglected. While this approximation can be shown to be justified for the coupling between bands in the relevant region of the spectrum between 1100 and 1800 cm^{-1}, the coupling to the intrinsically delocalized low-frequency vibrations might lead to additional anharmonic corrections. Here, our L-VSCF/L-VCI methodology can provide a starting point for a perturbative treatment of these couplings. Second, we have considered only fundamental vibrations, and overtones and combination bands as well as their coupling to the fundamentals have not been included. However, their treatment is straightforward within our L-VSCF/L-VCI methodology. Thus, beyond IR, Raman, and ROA spectroscopy, the L-VSCF/L-VCI methodology applied here also provides a natural starting point for the *first-principles* calculation of two-dimensional vibrational spectroscopies.[40]

While we have been able to address one of the challenges of theoretical vibrational spectroscopy for polypeptides and proteins by reliably assessing the importance of anharmonic corrections, several challenges remain. To compare the calculated spectra directly to experiment, it will be necessary to also address the inclusions of solvation effects and of the conformational flexibility of proteins. However, the results presented here show that it will be possible to tackle these challenges independently from the treatment of anharmonicities.

DOI: 10.1021/acs.jpclett.6b01451
J. Phys. Chem. Lett. 2016, 7, 3084−3090

COMPUTATIONAL METHODS

The optimized structures of the helical alanine polypeptides, namely 3_{10}-Ala_{10}, 3_{10}-Ala_{20}, and α-Ala_{20}, were adapted from refs 37 and 39, respectively. Therein and in this work all electronic structure calculations were performed using density-functional theory (DFT) with the TURBOMOLE program package.[41,42] The BP86 exchange-correlation functional,[43,44] with Ahlrichs' def-TZVP basis set,[45] along with the resolution-of-the-identity (RI) approximation and suitable auxiliary basis sets were used.[46,47] The normal modes and the required property tensor derivatives in the harmonic approximations were obtained with the SNF module of the MOVIPAC program package[48,49] employing the same computational methodology.

The anharmonic vibrational L-VSCF/L-VCI calculations were performed with our Python code VIBRATIONS,[27,28] which utilizes the VibTools[31,49] package for localizing the normal modes and the property tensor derivatives obtained with the SNF program. The anharmonic one-mode and two-mode potentials were calculated directly on 16-point grids, using the PYADF scripting framework[50] as an interface to TURBOMOLE. These calculations employed DFT/BP86/def-TZVP for the one-mode potentials and DFT/BP86/def2-TZVP[51] for the two-mode potentials. All vibrational spectra are plotted by convoluting the individual transitions with Lorentzian peaks with a full width at half-maximum of 15 cm^{-1}.

ASSOCIATED CONTENT

Supporting Information

The Supporting Information is available free of charge on the ACS Publications website at DOI: 10.1021/acs.jpclett.6b01451.

Theory of the calculation of IR, Raman, and ROA intensities in L-VSCF/L-VCI; details of the assignment of the normal modes to vibrational bands; and additional tests of the convergence of the VCI expansion for the amide III band in 3_{10}-Ala_{10} (PDF)

AUTHOR INFORMATION

Corresponding Author

*E-mail: c.jacob@tu-braunschweig.de.

Notes

The authors declare no competing financial interest.

ACKNOWLEDGMENTS

The authors are grateful to the Deutsche Forschungsgemeinschaft (DFG) for funding via Grant JA 2329-2/1 and acknowledge support from COST CMST-Action CM1405 Molecules in Motion (MOLIM). P.T.P. thanks Prof. Wim Klopper for his kind hospitality in his group at the Karlsruhe Institute of Technology (KIT).

REFERENCES

(1) Thielges, M. C.; Fayer, M. D. Protein Dynamics Studied with Ultrafast Two-Dimensional Infrared Vibrational Echo Spectroscopy. *Acc. Chem. Res.* **2012**, *45*, 1866−1874.

(2) Remorino, A.; Hochstrasser, R. M. Three-Dimensional Structures by Two-Dimensional Vibrational Spectroscopy. *Acc. Chem. Res.* **2012**, *45*, 1896−1905.

(3) Chruszcz-Lipska, K.; Blanch, E. W. Raman Optical Activity of Biological Samples. In *Optical Spectroscopy and Computational Methods in Biology and Medicine*; Baranska, M., Ed.; Challenges and Advances in Computational Chemistry and Physics 14; Springer: Netherlands, 2014; pp 61−81, DOI: 10.1007/978-94-007-7832-0_4.

(4) Ghosh, A.; Tucker, M. J.; Gai, F. 2D IR Spectroscopy of Histidine: Probing Side-Chain Structure and Dynamics via Backbone Amide Vibrations. *J. Phys. Chem. B* **2014**, *118*, 7799−7805.

(5) Herrmann, C.; Reiher, M. First-Principles Approach to Vibrational Spectroscopy of Biomolecules. In *Atomistic Approaches in Modern Biology*; Reiher, M., Ed.; Topics in Current Chemistry 268; Springer: Berlin, 2006; pp 85−132, DOI: 10.1007/128_2006_082.

(6) Luber, S.; Reiher, M. Theoretical Raman Optical Activity Study of the β-Domain of Rat Metallothionein. *J. Phys. Chem. B* **2010**, *114*, 1057−1063.

(7) Luber, S. Solvent Effects in Calculated Vibrational Raman Optical Activity Spectra of α-Helices. *J. Phys. Chem. A* **2013**, *117*, 2760−2770.

(8) Yamamoto, S.; Watarai, H.; Bouř, P. Monitoring the Backbone Conformation of Valinomycin by Raman Optical Activity. *ChemPhysChem* **2011**, *12*, 1509−1518.

(9) Yamamoto, S.; Kaminský, J.; Bouř, P. Structure and Vibrational Motion of Insulin from Raman Optical Activity Spectra. *Anal. Chem.* **2012**, *84*, 2440−2451.

(10) Reiher, M.; Neugebauer, J. A Mode-selective Quantum Chemical Method for Tracking Molecular Vibrations Applied to Functionalized Carbon Nanotubes. *J. Chem. Phys.* **2003**, *118*, 1634−1641.

(11) Kiewisch, K.; Neugebauer, J.; Reiher, M. Selective Calculation of High-intensity Vibrations in Molecular Resonance Raman Spectra. *J. Chem. Phys.* **2008**, *129*, 204103.

(12) Bouř, P.; Keiderling, T. A. Partial Optimization of Molecular Geometry in Normal Coordinates and Use as a Tool for Simulation of Vibrational Spectra. *J. Chem. Phys.* **2002**, *117*, 4126−4132.

(13) Ghysels, A.; Van Neck, D.; Van Speybroeck, V.; Verstraelen, T.; Waroquier, M. Vibrational Modes in Partially Optimized Molecular Systems. *J. Chem. Phys.* **2007**, *126*, 224102.

(14) Sahu, N.; Gadre, S. R. Vibrational Infrared and Raman Spectra of Polypeptides: Fragments-in-fragments Within Molecular Tailoring Approach. *J. Chem. Phys.* **2016**, *144*, 114113.

(15) Rauhut, G.; Pulay, P. Transferable Scaling Factors for Density Functional Derived Vibrational Force Fields. *J. Phys. Chem.* **1995**, *99*, 3093−3100.

(16) Katsyuba, S. A.; Zvereva, E. E.; Burganov, T. I. Is There a Simple Way to Reliable Simulations of Infrared Spectra of Organic Compounds? *J. Phys. Chem. A* **2013**, *117*, 6664−6670.

(17) Jacob, Ch. R.; Luber, S.; Reiher, M. Understanding the Signatures of Secondary-Structure Elements in Proteins with Raman Optical Activity Spectroscopy. *Chem. - Eur. J.* **2009**, *15*, 13491−13508.

(18) Christiansen, O. Vibrational Structure Theory: New Vibrational Wave Function Methods for Calculation of Anharmonic Vibrational Energies and Vibrational Contributions to Molecular Properties. *Phys. Chem. Chem. Phys.* **2007**, *9*, 2942−2953.

(19) Bowman, J. M.; Carrington, T.; Meyer, H.-D. Variational Quantum Approaches for Computing Vibrational Energies of Polyatomic Molecules. *Mol. Phys.* **2008**, *106*, 2145−2182.

(20) Christiansen, O. Selected New Developments in Vibrational Structure Theory: Potential Construction and Vibrational Wave Function Calculations. *Phys. Chem. Chem. Phys.* **2012**, *14*, 6672−6687.

(21) Pfeiffer, F.; Rauhut, G.; Feller, D.; Peterson, K. A. Anharmonic Zero Point Vibrational Energies: Tipping the Scales in Accurate Thermochemistry Calculations? *J. Chem. Phys.* **2013**, *138*, 044311.

(22) Roy, T. K.; Sharma, R.; Gerber, R. B. First-principles Anharmonic Quantum Calculations for Peptide Spectroscopy: VSCF Calculations and Comparison With Experiments. *Phys. Chem. Chem. Phys.* **2016**, *18*, 1607−1614.

(23) Daněček, P.; Kapitán, J.; Baumruk, V.; Bednárová, L.; Kopecký, V., Jr.; Bouř, P. Anharmonic Effects in IR, Raman, and Raman Optical Activity Spectra of Alanine and Proline Zwitterions. *J. Chem. Phys.* **2007**, *126*, 224513.

(24) Hudecová, J.; Profant, V.; Novotná, P.; Baumruk, V.; Urbanová, M.; Bouř, P. CH Stretching Region: Computational Modeling of Vibrational Optical Activity. *J. Chem. Theory Comput.* **2013**, *9*, 3096−3108.

DOI: 10.1021/acs.jpclett.6b01451
J. Phys. Chem. Lett. 2016, 7, 3084−3090

(25) Fornaro, T.; Biczysko, M.; Monti, S.; Barone, V. Dispersion Corrected DFT Approaches for Anharmonic Vibrational Frequency Calculations: Nucleobases and their Dimers. *Phys. Chem. Chem. Phys.* **2014**, *16*, 10112−10128.
(26) Barone, V.; Biczysko, M.; Bloino, J. Fully Anharmonic IR and Raman Spectra of Medium-size Molecular Systems: Accuracy and Interpretation. *Phys. Chem. Chem. Phys.* **2014**, *16*, 1759−1787.
(27) Panek, P. T.; Jacob, Ch. R. Efficient Calculation of Anharmonic Vibrational Spectra of Large Molecules with Localized Modes. *ChemPhysChem* **2014**, *15*, 3365−3377.
(28) Panek, P. T.; Jacob, Ch. R. On the Benefits of Localized Modes in Anharmonic Vibrational Calculations for Small Molecules. *J. Chem. Phys.* **2016**, *144*, 164111.
(29) Jung, J. O.; Gerber, R. B. Vibrational Wave Functions and Spectroscopy of (H2O)n, n = 2,3,4,5: Vibrational Self-consistent Field With Correlation Corrections. *J. Chem. Phys.* **1996**, *105*, 10332−10348.
(30) Carter, S.; Bowman, J. M.; Handy, N. C. Extensions and Tests of "multimode": a Code to Obtain Accurate Vibration/Rotation Energies of Many-mode Molecules. *Theor. Chem. Acc.* **1998**, *100*, 191−198.
(31) Jacob, Ch. R.; Reiher, M. Localizing Normal Modes in Large Molecules. *J. Chem. Phys.* **2009**, *130*, 084106.
(32) Cheng, X.; Steele, R. P. Efficient Anharmonic Vibrational Spectroscopy for Large Molecules Using Local-mode Coordinates. *J. Chem. Phys.* **2014**, *141*, 104105.
(33) Klinting, E. L.; König, C.; Christiansen, O. Hybrid Optimized and Localized Vibrational Coordinates. *J. Phys. Chem. A* **2015**, *119*, 11007−11021.
(34) König, C.; Hansen, M. B.; Godtliebsen, I. H.; Christiansen, O. FALCON: A method for flexible adaptation of local coordinates of nuclei. *J. Chem. Phys.* **2016**, *144*, 074108.
(35) Molina, A.; Smereka, P.; Zimmerman, P. M. Exploring the Relationship between Vibrational Mode Locality and Coupling Using Constrained Optimization. *J. Chem. Phys.* **2016**, *144*, 124111.
(36) Hanson-Heine, M. W. D. Intermediate Vibrational Coordinate Localization with Harmonic Coupling Constraints. *J. Chem. Phys.* **2016**, *144*, 204116.
(37) Jacob, Ch. R. Theoretical Study of the Raman Optical Activity Spectra of 310-Helical Polypeptides. *ChemPhysChem* **2011**, *12*, 3291−3306.
(38) Weymuth, T.; Jacob, Ch. R.; Reiher, M. A Local-Mode Model for Understanding the Dependence of the Extended Amide III Vibrations on Protein Secondary Structure. *J. Phys. Chem. B* **2010**, *114*, 10649−10660.
(39) Jacob, Ch. R.; Luber, S.; Reiher, M. Analysis of Secondary Structure Effects on the IR and Raman Spectra of Polypeptides in Terms of Localized Vibrations. *J. Phys. Chem. B* **2009**, *113*, 6558−6573.
(40) Hanson-Heine, M. W. D.; Husseini, F. S.; Hirst, J. D.; Besley, N. A. Simulation of Two-Dimensional Infrared Spectroscopy of Peptides Using Localized Normal Modes. *J. Chem. Theory Comput.* **2016**, *12*, 1905−1918.
(41) Turbomole V6.3 2011, a Development of University of Karlsruhe and Forschungszentrum Karlsruhe GmbH, 1989−2007, Turbomole GmbH, since 2007; available from http://www.turbomole.com.
(42) Ahlrichs, R.; Bär, M.; Häser, M.; Horn, H.; Kölmel, C. Electronic Structure Calculations on Workstation Computers: The Program System Turbomole. *Chem. Phys. Lett.* **1989**, *162*, 165−169.
(43) Becke, A. D. Density-functional Exchange-energy Approximation with Correct Asymptotic Behavior. *Phys. Rev. A: At., Mol., Opt. Phys.* **1988**, *38*, 3098−3100.
(44) Perdew, J. P. Density-functional Approximation for the Correlation Energy of the Inhomogeneous Electron Gas. *Phys. Rev. B: Condens. Matter Mater. Phys.* **1986**, *33*, 8822−8824.
(45) Schäfer, A.; Huber, C.; Ahlrichs, R. Fully Optimized Contracted Gaussian Basis Sets of Triple Zeta Valence Quality for Atoms Li to Kr. *J. Chem. Phys.* **1994**, *100*, 5829−5835.
(46) Eichkorn, K.; Treutler, O.; Öhm, H.; Häser, M.; Ahlrichs, R. Auxiliary Basis Sets to Approximate Coulomb Potentials. *Chem. Phys. Lett.* **1995**, *240*, 283−289.
(47) Eichkorn, K.; Treutler, O.; Öhm, H.; Häser, M.; Ahlrichs, R. Auxiliary Basis Sets to Approximate Coulomb Potentials. *Chem. Phys. Lett.* **1995**, *240*, 283−289.
(48) Neugebauer, J.; Reiher, M.; Kind, C.; Hess, B. A. Quantum Chemical Calculation of Vibrational Spectra of Large Molecules-Raman and IR Spectra for Buckminsterfullerene. *J. Comput. Chem.* **2002**, *23*, 895−910.
(49) Weymuth, T.; Haag, M. P.; Kiewisch, K.; Luber, S.; Schenk, S.; Jacob, Ch. R.; Herrmann, C.; Neugebauer, J.; Reiher, M. MoViPac: Vibrational Spectroscopy with a Robust Meta-program for Massively Parallel Standard and Inverse Calculations. *J. Comput. Chem.* **2012**, *33*, 2186−2198.
(50) Jacob, Ch. R.; Beyhan, S. M.; Bulo, R. E.; Gomes, A. S. P.; Götz, A. W.; Kiewisch, K.; Sikkema, J.; Visscher, L. PyADF − A Scripting Framework for Multiscale Quantum Chemistry. *J. Comput. Chem.* **2011**, *32*, 2328−2338.
(51) Weigend, F.; Ahlrichs, R. Balanced Basis Sets of Split Valence, Triple Zeta Valence and Quadruple Zeta Valence Quality for H to Rn: Design and Assessment of Accuracy. *Phys. Chem. Chem. Phys.* **2005**, *7*, 3297−3305.

DOI: 10.1021/acs.jpclett.6b01451
J. Phys. Chem. Lett. 2016, 7, 3084−3090